Exchange bias effect in bulk multiferroic $BiFe_{0.5}Sc_{0.5}O_3$

Cite as: AIP Advances 10, 045102 (2020); doi: 10.1063/1.5135586
Submitted: 6 November 2019 • Accepted: 11 March 2020 •
Published Online: 1 April 2020

View Online Export Citation CrossMark

E. L. Fertman,[1] A. V. Fedorchenko,[1] V. A. Desnenko,[1] V. V. Shvartsman,[2] D. C. Lupascu,[2] S. Salamon,[3] H. Wende,[3] A. I. Vaisburd,[4] A. Stanulis,[5,6] R. Ramanauskas,[5] N. M. Olekhnovich,[7] A. V. Pushkarev,[7] Yu. V. Radyush,[7] D. D. Khalyavin,[8] and A. N. Salak[9,a)]

AFFILIATIONS

[1]B. Verkin Institute for Low Temperature Physics and Engineering of NASU, Nauky 47, Kharkov 61103, Ukraine
[2]Institute for Materials Science and Center for Nanointegration Duisburg-Essen (CENIDE), University of Duisburg-Essen, Essen 45141, Germany
[3]Faculty of Physics and Center for Nanointegration Duisburg-Essen (CENIDE), University of Duisburg-Essen, Duisburg 47057, Germany
[4]V. N. Karazin Kharkiv National University, 4 Svobody Sq., Kharkiv 61000, Ukraine
[5]Department of Electrochemical Materials Science, Center for Physical Sciences and Technology, Sauletekio Av. 3, Vilnius LT-10257, Lithuania
[6]Energy Safety Research Institute (ESRI), College of Engineering, Swansea University, Bay Campus, Fabian Way, Swansea SA1 8EN, United Kingdom
[7]Scientific-Practical Materials Research Centre of NASB, P. Brovka 19, Minsk 220072, Belarus
[8]ISIS Facility, Rutherford Appleton Laboratory, Chilton, Didcot, Oxfordshire OX11 0QX, United Kingdom
[9]Department of Materials and Ceramics Engineering, CICECO-Aveiro Institute of Materials, University of Aveiro, Aveiro 3810-193, Portugal

[a)]**Author to whom correspondence should be addressed:** salak@ua.pt

ABSTRACT

Below the Néel temperature, T_N ~ 220 K, at least two nano-scale antiferromagnetic (AFM) phases coexist in the polar polymorph of the $BiFe_{0.5}Sc_{0.5}O_3$ perovskite; one of these phases is a weak ferromagnetic. Non-uniform structure distortions induced by high-pressure synthesis lead to competing AFM orders and a nano-scale spontaneous magnetic phase separated state of the compound. Interface exchange coupling between the AFM domains and the weak ferromagnetic domains causes unidirectional anisotropy of magnetization, resulting in the exchange bias (EB) effect. The EB field, H_{EB}, and the coercive field strongly depend on temperature and the strength of the cooling magnetic field. H_{EB} increases with an increase in the cooling magnetic field and reaches a maximum value of about 1 kOe at 5 K. The exchange field vanishes above T_N with the disappearance of long-range magnetic ordering. The effect is promising for applications in electronics as it is large enough and as it is tunable by temperature and the magnetic field applied during cooling.

© 2020 Author(s). All article content, except where otherwise noted, is licensed under a Creative Commons Attribution (CC BY) license (http://creativecommons.org/licenses/by/4.0/). https://doi.org/10.1063/1.5135586

I. INTRODUCTION

Multiferroic materials with polar and magnetic orders combine spontaneous magnetization and electric polarization and offer a unique opportunity to effectively cross-control these parameters. Therefore, the search for new multiferroics has attracted the attention of many research groups worldwide.[1–3]

The compositions derived from the "classical" type-I multiferroic $BiFeO_3$ are the best studied materials.[4,5] Cation substitutions in the crystallographic positions of bismuth result mainly in a change

© Author(s) 2020

in the temperature of the ferroelectric transition, while the iron-site substitutions allow variation of the magnetic transition. Using conventional synthesis routes, it is usually possible to achieve only 10–15 mol. % of substitution of iron in bismuth ferrite by other B^{3+} cations even when the size difference between Fe^{3+} and a substituent is not big. Application of the high-pressure (HP) synthesis technique enables one to produce single-phase $Bi(Fe, B^{3+})O_3$ solid solutions over a wide compositional range and obtain new bulk perovskite phases that cannot be formed at ambient pressure.[6–10] Moreover, it has been recently shown that the post-synthesis thermal treatment of high-pressure stabilized phases can result in formation of novel phases via annealing-stimulated irreversible phase transformations (*conversion polymorphism of metastable phases*).[11,12]

Using HP synthesis, a metastable equimolar solid solution between bismuth ferrite and bismuth scandate, namely, $BiFe_{0.5}Sc_{0.5}O_3$, which is the focus of the present study, was produced.[13] The as-prepared perovskite $BiFe_{0.5}Sc_{0.5}O_3$ phase is the antipolar *Pnma* polymorph that can be irreversibly converted to the polar *Ima*2 one by annealing within a temperature range of 820–920 K at ambient pressure. Long-range antiferromagnetic (AFM) ordering with a weak ferromagnetic (FM) component was found in both *Pnma* and *Ima*2 polymorphs of $BiFe_{0.5}Sc_{0.5}O_3$ below the Néel temperature, $T_N \sim 220$ K.[13] Besides, the polar *Ima*2 modification is a rare case of canted ferroelectrics, which combines both ferroelectric- and antiferroelectric-like displacements of cations along different crystallographic axes. This polymorph definitely deserves a detailed study. We have recently reported unusual magnetic properties of this material, which were associated with its glassy magnetic behavior and two distinct (linear and non-linear) contributions to the total magnetic moment. The non-linear contribution was found to be extremely sensitive to the applied magnetic field.[14] In order to clarify the nature of these contributions, a series of complementary magnetic measurements was undertaken. The main objective of such an extended study was to detect an exchange bias (EB) effect, which is direct evidence of the magnetic phase-segregated state.

The EB effect manifests itself as a shift in a magnetic hysteresis loop along the magnetic field axis when the sample is cooled in the presence of a magnetic field below the magnetic ordering temperatures. The effect is caused by an exchange interaction at the interface between different magnetic phases, which induces an additional unidirectional anisotropy of magnetization.[15–18] Exchange bias has been observed in various magnetic systems at the interfaces between the magnetic phases such as ferromagnetic, antiferromagnetic, ferrimagnetic, and spin glass. Among these systems, the ferromagnetic/antiferromagnetic bilayers are the most explored.[19] The EB phenomenon has been widely studied because of its importance in spintronic applications as a magnetic random-access memory and as spin valves.[20,21] It should be noticed that the EB effect has been observed not only in artificially prepared systems like bilayers but also in spontaneously phase-segregated compounds. At relatively high temperature, these compounds exist as single-phase systems. However, due to phase transformations at a lower temperature, they split into different coexisting magnetic phases (i.e., they become phase segregated). For instance, the spontaneously phase segregated perovskites $Pr_{2/3}Ca_{1/3}MnO_3$ and $Nd_{2/3}Ca_{1/3}MnO_3$ are composed of FM nanodomains immersed in a charge-ordered AFM host matrix.[22,23] Exchange coupling at interfaces between the FM domains and the surrounding AFM matrix causes a unidirectional anisotropy of magnetization that results in the EB effect.

Possible applications as well as fundamental interest have motivated researchers to seek for the EB phenomenon in new crystalline phases. Here, we report on a detailed study of the EB effect in the polar *Ima*2 polymorph of the metastable $BiFe_{0.5}Sc_{0.5}O_3$ perovskite and demonstrate that the effect is associated with nano-sized magnetic phase separation in this material.

II. EXPERIMENTAL DETAILS

Dense homogeneous ceramics of the $BiFe_{0.5}Sc_{0.5}O_3$ composition were synthesized under high-pressure from the precursor prepared via a sol-gel combustion route. Details of the precursor preparation and the high-pressure synthesis can be found in Ref. 24 and the supplementary material.

The obtained ceramic samples were annealed in air at 870 K for 3 h to ensure a complete transformation from the as-synthesized antipolar *Pnma* phase to the polar *Ima*2 phase. Phase analysis of the samples was performed using a PANalytical X'Pert Powder x-ray diffractometer (XRD, Ni-filtered Cu Kα radiation) at room temperature. The microstructure of fractured surfaces of the samples was studied using a Hitachi S-4100 scanning electron microscope (SEM).

Magnetic properties of the samples were measured in the range of 5–300 K using the vibrating sample magnetometry (VSM) option of a Quantum Design PPMS DynaCool system. Temperature dependent data were collected both in zero-field-cooled (ZFC) and field-cooled (FC) modes in the applied field up to 20 kOe. Magnetic hysteresis loops, $M(H)$, were measured at different temperatures below 250 K between −20 kOe and 20 kOe under both ZFC and FC conditions. Before each measurement, the samples were warmed to 320 K and kept at this temperature for 30 min to ensure demagnetization. For ZFC experiments, the samples were cooled in a zero magnetic field from room temperature to the measuring temperatures. For FC experiments, the sample was cooled in different magnetic fields, H_{cool}, from 0.8 kOe to 20 kOe, while temperature was changed in the same way as in the case of ZFC experiments.

III. RESULTS AND DISCUSSION

According to both SEM observations and XRD study, as well as the neutron diffraction data measured in a wide temperature range,[13] the annealed $BiFe_{0.5}Sc_{0.5}O_3$ ceramics were homogeneous and single-phase with the polar *Ima*2 perovskite structure. Below $T_N \sim 220$ K, the *dc* magnetic moment of the samples rapidly increases, indicating an onset of the antiferromagnetic order with a weak ferromagnetic component (see the supplementary material for more details).

The $M(H)$ dependences measured below T_N show hysteresis with a weak ferromagnetic contribution to the total magnetization. All loops recorded after ZFC turned out to be centered about the origin of coordinates H and M (Fig. S3 in the supplementary material), while the loops after FC are shifted to the negative direction of the H-axis (Fig. 1). Such a shift indicates an exchange bias effect with the EB field, H_{EB}, and the coercive field, H_c, defined as

$$H_{EB} = (H_1 + H_2)/2, \quad (1)$$

© Author(s) 2020

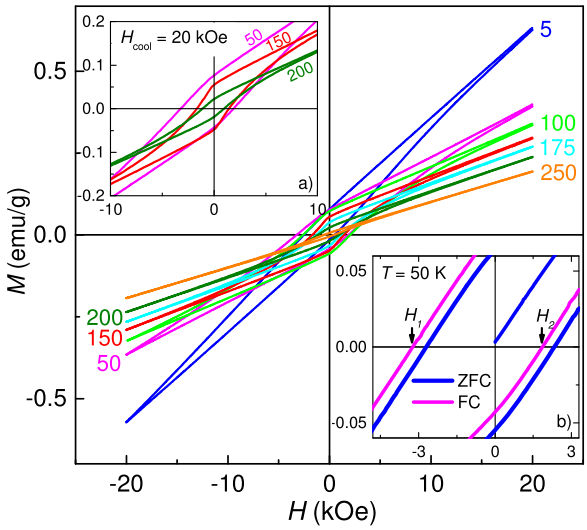

FIG. 1. Magnetic hysteresis loops for the polar $BiFe_{0.5}Sc_{0.5}O_3$ polymorph measured after the FC procedure [the numbers denote the temperature values (in Kelvin)]: (a) the hysteresis loops measured after the FC procedure at 50 K, 150 K, and 200 K and (b) the magnified central region of the hysteresis loops at 50 K measured after ZFC and FC (H_{cool} = 20 kOe).

and

$$H_C = (H_2 - H_1)/2, \quad (2)$$

respectively. Here, H_1 and H_2 are the magnetic field values that correspond to the zero M value for decreasing and increasing field branches of the hysteresis loops. As seen from the inset in Fig. 1, for the sample cooled down to 50 K in the magnetic field H_{cool} = 20 kOe, H_1 and H_2 are −3.24 kOe and 1.87 kOe, respectively. The EB field and the coercive field calculated using Eqs. (1) and (2) are H_{EB} ~ −0.69 kOe and H_c ~ 2.56 kOe, respectively.

The value of the EB field in $BiFe_{0.5}Sc_{0.5}O_3$ strongly depends both on temperature (Fig. 2) and the cooling magnetic field (Fig. 3). H_{EB} increases non-linearly with decreasing temperature and reaches ~1 kOe at 5 K (at H_{cool} = 20 kOe) (Fig. 2). This H_{EB} value is about 65% of the corresponding coercive field. Similarly, at a fixed temperature, the magnitude of H_{EB} increases as the cooling field is increased. One can see from Fig. 3 that at 5 K, $H_{EB}(H_{cool})$ increases fast at low values of the cooling field but changes slowly at H_{cool} > 15 kOe, reaching a maximum absolute value of H_{EB} ~ 1 kOe at H_{cool} = 20 kOe. For zero cooling field, H_{EB} = 0.

The measurements performed on a sample of the antipolar *Pnma* modification of $BiFe_{0.5}Sc_{0.5}O_3$ gave a maximum value of the EB field of 46 Oe, which is about a factor of 20 lower than that in the polar polymorph under the same conditions of H_{cool} and temperature. At the same time, the FC magnetization measured at 5 K is smaller in the polar polymorph than in the antipolar one (cf. ~0.02 emu/g vs ~0.09 emu/g).[13]

The observed EB effect denotes unidirectional exchange interaction anisotropy, driving the FM moments back to their initial orientations when the magnetic field is removed. As mentioned, the EB effect is caused by the exchange interaction at the interface of coexisting phases of a different magnetic nature.

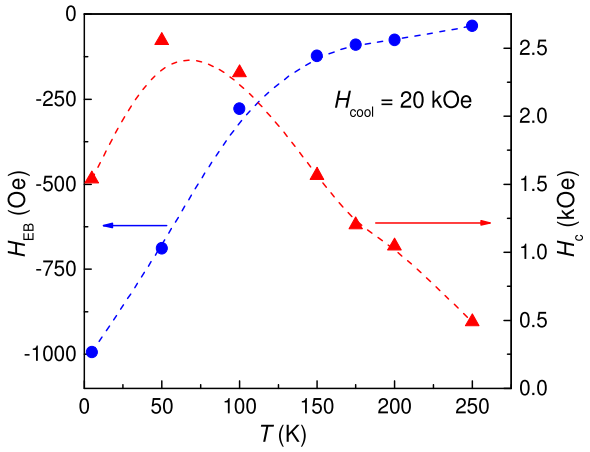

FIG. 2. The temperature dependences of the exchange bias field, $H_{EB}(T)$, and the coercive field, $H_c(T)$, at H_{cool} = 20 kOe. The lines between the points are guides to the eye.

We have recently demonstrated for particular temperatures[14] that the field dependence of magnetization of this material, $M(H)$, is best fitted as a sum of two contributions only, $M_1(H) + M_2(H)$. The first (non-linear to the applied field) term, described by a Langevin function, is considered to be an FM contribution to the total magnetic moment of $BiFe_{0.5}Sc_{0.5}O_3$, while the second (linear) term, $M_2 = \chi H$, is an AFM contribution (supplementary material). Based on this approach, the temperature dependent FM contribution to the total magnetization, $M_{FM}(T)$, was calculated (Fig. 4). The shape of the obtained $M_{FM}(T)$ plot agrees well with that of the experimental ZFC $M(T)$ curve (supplementary material) and the temperature dependent coercive field curve $H_c(T)$ (see Fig. 2). When comparing the curves, one should take into account that the position of the maximum depends on the value of the magnetic field applied. The H_{EB} value increases with the decrease in the FM contribution to the total magnetization (Fig. 2).

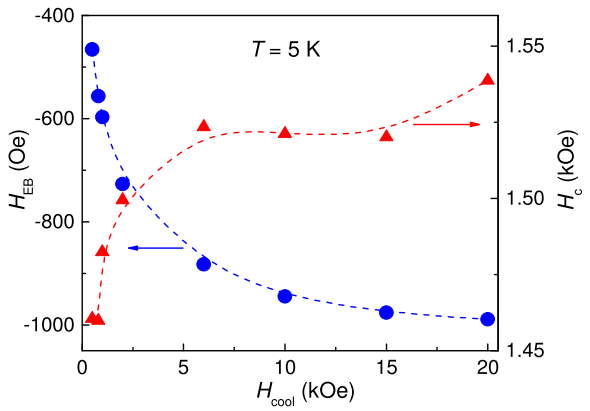

FIG. 3. Cooling field dependences of the exchange bias field, $H_{EB}(H_{cool})$, and the coercive field, $H_c(H_{cool})$, at 5 K. The lines between the points are guides to the eye.

© Author(s) 2020

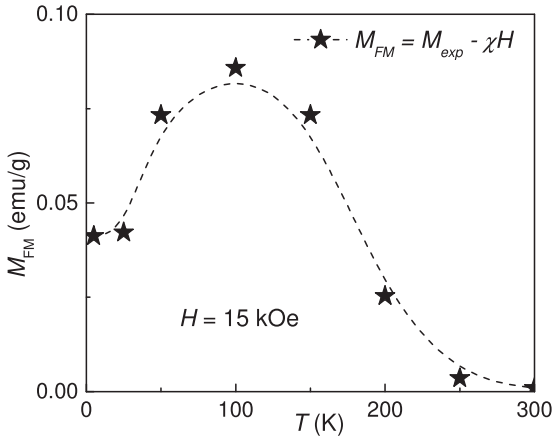

FIG. 4. The FM contribution, M_{FM}, obtained by subtracting the AFM contribution, χH, from the total experimental magnetic moment, M_{exp}, as a function of temperature. The line between the points is a guide to the eye.

A sharp increase in the absolute value of the EB field below about 150 K (Fig. 2) agrees well with the decrease in the FM contribution and a decrease in the coercive field below this temperature (Fig. 3). These data seem to be consistent with the Meiklejohn model evaluation of H_{EB} in a two layer AFM–FM system,[15] $H_{EB} \approx J_{ex}/(M_{FM} \times t_{FM})$, where J_{ex} is the FM/AFM exchange interaction constant per unit area, and M_{FM} and t_{FM} are the magnetization and thickness of the FM layer, respectively. The lower H_{EB} value observed in the antipolar polymorph in comparison with that in the polar one conforms to the Meiklejohn model as the antipolar polymorph demonstrates a higher M_{FM} value.

Based on these results, we suggest that the exchange bias effect in the studies manifests a coexistence between AFM and weak FM regions. Usually, it is related to a core–shell structure of nanoparticles[25] or compositional segregation.[26,27]

Huang *et al.* reported on the exchange bias effect in $BiFeO_3$ nanoparticles that demonstrate a natural core–shell structure.[25] The exchange interaction in such a material was shown to occur between the frozen surface spins and the "core" spins. It was demonstrated that this EB effect in $BiFeO_3$ is scale-dependent and exhibits itself only when the nanoparticles are as small as 18 nm in diameter. The $BiFe_{0.5}Sc_{0.5}O_3$ ceramics are certainly not nanostructured (see Fig. S1 in the supplementary material). Therefore, in the ceramics under study, a shell contribution (if any) is negligible in comparison with the volume AFM contribution.

Belik has observed an EB effect in high-pressure synthesized $BiFe_{1-x}Mn_xO_3$ ceramics.[26] In many respects, this material is very close to $BiFe_{0.5}Sc_{0.5}O_3$. Belik associated the tunable EB effect in $BiFe_{0.6}Mn_{0.4}O_3$ with "extrinsic" reasons, such as the presence of magnetic impurities (a real extrinsic origin) or sample inhomogeneities or even surface effects (a pseudo-extrinsic origin). The magnetization loop obtained in $BiFe_{0.6}Mn_{0.4}O_3$ was of a butterfly-like shape, which is a certain indication of magnetic impurity(ies). However, no butterfly-like loops has been observed in our case. Besides, the detailed neutron diffraction study between 1.5 K and 300 K revealed no other magnetic phase except for antipolar *Pnma* or polar *Ima*2 in the as-prepared and the annealed samples of $BiFe_{0.5}Sc_{0.5}O_3$, respectively. Therefore, the presence of a magnetic phase with a nature different from the weak ferromagnetism driven by the Dzyaloshinskii–Moria antisymmetric exchange in the antiferromagnetic $BiFe_{0.5}Sc_{0.5}O_3$[13] can be ruled out. Nevertheless, the exchange bias phenomenon, which is a strong interface effect, certainly manifests itself in the polar phase of $BiFe_{0.5}Sc_{0.5}O_3$. This suggests that the EB effect is intrinsic to this material and is likely caused by local magnetic heterogeneities.

These local magnetic heterogeneities may manifest themselves in a spin-glass like behavior, which is attributed to magnetic ordering frustration resulting from a local random competition between antiferromagnetic and ferromagnetic interactions.[28] The spin-glass behavior was reported both in unmodified[1] and in doped BFO.[29] In the recently reported case, the competing AFM–FM interactions are related to a partial reduction in Fe^{3+} to Fe^{2+}.[29] We have also observed a spin-glass like behavior in $BiFe_{0.5}Sc_{0.5}O_3$ with a characteristic cusp anomaly on the ZFC curve at approximately 150 K (Fig. S2), i.e., at the same temperature, below which the exchange bias field starts increasing sharply. The spin-glass like behavior is another manifestation of the coexistence of FM and AFM ordered regions.[30]

Thus, despite structural homogeneity, we deal with nanoscale magnetic phase segregation. It is likely that two antiferromagnetic nano-size phases, not resolved in neutron scattering, coexist in the polar $BiFe_{0.5}Sc_{0.5}O_3$ polymorph with one of the phases being a weak ferromagnetic. Ceramics of high-pressure stabilized phases are under mechanical stress since such a phase is obtained by quenching.[12] Moreover, such a stress is not homogeneous that can result in suppression of the weak ferromagnetism in some domains. This is in agreement with results of our previous study, indicating that magnetic properties of $BiFe_{0.5}Sc_{0.5}O_3$ are very sensitive to the applied uniaxial pressure.[14] Another origin of nanoscale magnetic phase segregation can be the non-homogenous distribution of *B*-site cations. In Sc-rich regions, the Dzyaloshinskii–Moriya interaction and the resulting weak ferromagnetism can be suppressed. Besides, exchange bias can arise on the border between these regions and the Fe-rich regions. Further studies will be necessary to prove or disprove these assumptions.

IV. CONCLUSION

The high-pressure stabilized multiferroic $BiFe_{0.5}Sc_{0.5}O_3$ perovskite exhibits antiferromagnetic ordering with a weak ferromagnetic component. Below the Néel temperature, $T_N \sim 220$ K, an exchange bias effect, which can be tuned by the cooling magnetic field and temperature, has been revealed. The observed EB is intrinsic to this material and is evident of a local magnetic inhomogeneity associated with a nanoscale magnetic phase segregated state. We assume that two antiferromagnetic phases coexist in this material and one of the AFM phases is a weak ferromagnetic. Exchange coupling at interfaces between the AFM domains and weak ferromagnetic domains causes unidirectional anisotropy of magnetization, resulting in the EB effect. The effect is sufficiently large at easily accessible temperatures and, provided enhancement and optimization via chemical modification of the material, has potential for practical application.

© Author(s) 2020

SUPPLEMENTARY MATERIAL

See the supplementary material for details of the precursor preparation and the high-pressure synthesis, the SEM observations, the XRD study, and results of the preliminary magnetic measurements, as well as the equations used for calculation of the field dependent magnetization.

ACKNOWLEDGMENTS

This work was supported by the TUMOCS project. This project has received funding from the European Union Horizon 2020 Research and Innovation Programme under Marie Skłodowska-Curie Grant Agreement No. 645660. The research done in University of Aveiro was supported by the project CICECO-Aveiro Institute of Materials, UIDB/50011/2020 & UIDP/50011/2020, financed by national funds through the Portuguese Foundation for Science and Technology/MCTES. Financial support by the DFG via FOR 1509 (WE2623/13), CRC 1242 (Project No. 278162697, sub-project A05) and CRC/TRR 247 (Project No. 388390466, sub-project B02) is gratefully acknowledged.

REFERENCES

[1] G. Catalan and J. F. Scott, Adv. Mater. **21**, 2463 (2009).
[2] A. P. Pyatakov and A. K. Zvezdin, Phys.-Usp. **55**, 557 (2012).
[3] C. Daumont, J. Wolfman, C. Autret-Lambert, P. Andreazza, and B. Negulescu, Appl. Phys. Lett. **112**, 112401 (2018).
[4] D. C. Arnold, IEEE Trans. Ultrason., Ferroelectr., Freq. Control **62**, 62 (2015).
[5] J. A. Quintana-Cilleruelo, V. K. Veerapandiyan, M. Deluca, M. Algueró, and A. Castro, Materials **12**, 1515 (2019).
[6] M. R. Suchomel, C. I. Thomas, M. Allix, M. J. Rosseinsky, and A. M. Fogg, Appl. Phys. Lett. **90**, 112909 (2007).
[7] P. Mandal, A. Sundaresan, C. N. R. Rao, A. Iyo, P. M. Shirage, Y. Tanaka, Ch. Simon, V. Pralong, O. I. Lebedev, V. Caignaert, and B. Raveau, Phys. Rev. B **82**, 100416(R) (2010).
[8] K. Oka, T. Koyama, T. Ozaaki, S. Mori, Y. Shimakawa, and M. Azuma, Angew. Chem., Int. Ed. **51**, 7977 (2012).
[9] A. Belik, D. A. Rusakov, T. Furubayashi, and E. Takayama-Muromachi, Chem. Mater. **24**, 3056 (2012).
[10] A. N. Salak, D. D. Khalyavin, A. V. Pushkarev, Yu. V. Radyush, N. M. Olekhnovich, A. D. Shilin, and V. V. Rubanik, J. Solid State Chem. **247**, 90 (2017).
[11] A. N. Salak, D. D. Khalyavin, E. Eardley, N. M. Olekhnovich, A. V. Pushkarev, Yu. V. Radyush, A. D. Shilin, and V. V. Rubanik, Crystals **8**, 00091 (2018).
[12] D. D. Khalyavin, A. N. Salak, E. L. Fertman, O. V. Kotlyar, E. Eardley, N. M. Olekhnovich, A. V. Pushkarev, Yu. V. Radyush, A. V. Fedorchenko, V. A. Desnenko, P. Manuel, L. Ding, E. Čižmár, and A. Feher, Chem. Commun. **55**, 4683 (2019).
[13] D. D. Khalyavin, A. N. Salak, N. M. Olekhnovich, A. V. Pushkarev, Yu. V. Radyush, P. Manuel, I. P. Raevski, M. L. Zheludkevich, and M. G. S. Ferreira, Phys. Rev. B **89**, 174414 (2014).
[14] A. V. Fedorchenko, E. L. Fertman, A. N. Salak, V. A. Desnenko, E. Čižmár, A. Feher, A. I. Vaisburd, N. M. Olekhnovich, A. V. Pushkarev, Yu. V. Radyush, A. Zarkov, and A. Kareiva, J. Magn. Magn. Mater. **465**, 328 (2018).
[15] W. H. Meiklejohn and C. P. Bean, Phys. Rev. **102**, 1413 (1956).
[16] J. Nogués and I. K. Schuller, J. Magn. Magn. Mater. **192**, 203 (1999).
[17] S. Giri, M. Patra, and S. Majumdar, J. Phys.: Condens. Matter **23**, 073201 (2011).
[18] A. S. Moskvin, J. Magn. Magn. Mater. **463**, 50 (2018).
[19] Q. Xu, Y. Sheng, X. Xue, X. Yuan, Z. Wen, and J. Du, Jpn. J. Appl. Phys., Part 1 **53**, 08NM01 (2014).
[20] C. Binasch, P. Grünberg, F. Saurenbach, and W. Zinn, Phys. Rev. B **39**, 4828 (1989).
[21] F. Radu, R. Abrudan, I. Radu, D. Schmitz, and H. Zabel, Nat. Commun. **3**, 715 (2012).
[22] D. Niebieskikwiat and M. B. Salamon, Phys. Rev. B **72**, 174422 (2005).
[23] E. Fertman, S. Dolya, V. Desnenko, L. A. Pozhar, M. Kajňaková, and A. Feher, J. Appl. Phys. **115**, 203906 (2014).
[24] E. L. Fertman, A. V. Fedorchenko, D. D. Khalyavin, A. N. Salak, A. Baran, V. A. Desnenko, O. V. Kotlyar, E. Čižmár, A. Feher, E. S. Syrkin, A. I. Vaisburd, N. M. Olekhnovich, A. V. Pushkarev, Yu. V. Radyush, A. Stanulis, and A. Kareiva, J. Magn. Magn. Mater. **429**, 177 (2017).
[25] F. Huang, X. Xu, X. Lu, M. Zhou, H. Sang, and J. Zhu, Sci. Rep. **8**, 2311 (2018).
[26] A. A. Belik, Inorg. Chem. **52**, 2015 (2013).
[27] X. Hai, W. F. Liu, Y. F. Gong, H. Zhang, P. Wu, S. Y. Wanng, and G. H. Rao, Int. J. Mod. Phys. B **28**, 1350194 (2014).
[28] S. Kirckpatrick and D. Sherrington, Phys. Rev. B **17**, 4384 (1978).
[29] K. C. Verma and R. K. Kotnala, RSC Adv. **6**, 57727 (2016).
[30] M. Gruyters, Phys. Rev. B **79**, 134415 (2009).

© Author(s) 2020